Available online at www.sciencedirect.com
SCIENCE DIRECT®
Minerals Engineering 19 (2006) 340–347
MINERALS ENGINEERING
This article is also available online at: www.elsevier.com/locate/mineng

Mechanical activation of olivine

R.A. Kleiv *, M. Thornhill

Department of Geology and Mineral Resources Engineering, Norwegian University of Science and Technology, Sem Sælandsvei 1, N-7491 Trondheim, Norway

Received 15 July 2005; accepted 14 August 2005
Available online 13 October 2005

Abstract

This paper investigates how mechanical activation of olivine can increase the mineral's surface reactivity, and illustrates how such technology can give rise to new or improved olivine products. The olivine material used in this study consisted of pure olivine crystals ($Mg_{1.860}Fe_{0.134}Ni_{0.006}SiO_4$) originating from North Cape Minerals dunite deposit at Åheim in Western Norway. Following activation in a planetary mono mill, the activated olivine products were visually inspected using scanning electron microscopy (SEM) and characterised with respect to particle size, specific surface area (BET) and X-ray diffraction (XRD) signature. The surface reactivity of the activated olivine products was determined through simple acid leaching experiments in which the initial acid consumption rates were determined. The initial phase of olivine dissolution could be modelled using first order kinetics. Prolonged dry milling of pure olivine crystals resulted in highly aggregated products that were more reactive with respect to dissolution in acid than their respective BET surface areas would suggest. Relative to olivine that had been milled for 1 min, 60 min of milling increased the initial reaction rate by a factor of 9.0, whereas the corresponding increase in specific surface area was 1.8. The results from both the leaching experiments and the XRD analysis suggest that the observed over-proportional increase in reactivity with respect to surface area is largely due to structural disordering (i.e. mechanical activation) of the olivine surfaces.

Keywords: Mechanical activation; Grinding; Leaching; Reaction kinetics; Industrial minerals

1. Introduction

Although the use of mechanical activation in mineral processing has found its main application within the field of extractive metallurgy where the technology has been employed as a pre-treatment step prior to the subsequent extraction of metallic ores (Baláž, 2000, 2003 and references within), several applications and concepts have been proposed utilising industrial minerals (Kleiv and Sandvik, 2005). In addition to increasing mineral dissolution rates, mechanical activation can also be employed in order to improve the kinetics of adsorption, catalysis and mineral synthesis, as well as to customize the mineral surfaces with respect to structure and composition. Modifying the structure, composition and reactivity of the mineral surface could give rise to new applications and products.

This paper provides an initial assessment of the potential increase of olivine surface reactivity that can be achieved through mechanical activation, and is, as far as the authors are aware, the first to investigate the properties of mechanically activated olivine. Whereas the value of olivine for traditional uses like slag conditioner, refractory materials, foundry sands and blasting sands is based on the mineral's bulk chemistry and favourable mechanical properties (Rudi, 2001; Harben, 2002; Kleiv et al., 2002), a number of new uses are now emerging where the potential value is closely linked to the reactivity of the olivine surface.

The use of olivine for carbon dioxide sequestration represents one potential application of the mineral in which

* Corresponding author.
E-mail address: rolf.kleiv@geo.ntnu.no (R.A. Kleiv).

0892-6875/$ - see front matter © 2005 Elsevier Ltd. All rights reserved.
doi:10.1016/j.mineng.2005.08.008

the process and products could benefit from mechanical activation. Carbonation of free magnesium ions is an exothermic process, thermodynamically favoured at low temperatures and high pressure (Huijgen and Comans, 2003; Lackner et al., 1995, 1997). Unfortunately, this is not the case for the solubility and surface reactivity of the magnesium silicates, which exhibit a strong positive correlation with temperature. However, mechanical activation could significantly improve the reaction kinetics. This was shown by O'Connor et al. (2001) who used attrition as a pre-treatment step when using serpentine as a sequestration agent at room temperature and a pressure of 10 bar. Their conversion rates were comparable to those obtained for non-activated mafic and ultramafic minerals at considerably higher temperatures and pressure. Other studies (Kalinkina et al., 2001a,b; Kalinkin et al., 2003) have demonstrated that prolonged milling can cause the uptake of significant amounts of carbon dioxide even when the gas is present at standard atmospheric conditions.

The utilisation of olivine's capacity to neutralise sulphuric acid has been described by several investigators (Schuiling, 1986, 1998; Jonckbloedt, 1998; Kleiv et al., 2001; Morales and Herbert, 2001; Kleiv and Thornhill, 2002). Due to the high solubility of magnesium sulphate, the use of olivine as a neutralising agent will not result in voluminous sulphate precipitates. This can be a problem when using calcite as the calcium ions leached from the mineral combine with sulphate ions to form gypsum. Calcite, however, is usually seen as the better choice due to its higher reactivity and more favourable dissolution kinetics. As will be shown in this paper, prolonged energy-intensive milling can cause a substantial increase in the olivine dissolution rate. This would also be beneficial for the use of olivine as a magnesium source for agricultural soil improvement, which represents yet another example of a potentially valuable product for which the reactivity of the mineral surface is a key parameter. Others include olivine as a heavy metal adsorbent (Kleiv, 2001; Kleiv and Sandvik, 2002; Kleiv and Thornhill, 2004), as an additive and chemical substitute in water treatment, as well as catalysts for decomposition of toxic organic chemicals in deposited waste or sediments.

The relative increase in reactivity as a function of milling/activation time will depend on the reaction in question. In other words, the possibilities of improving the adsorption kinetics with respect to heavy metals or carbon dioxide could differ from those found for the dissolution of olivine in acid. It is the latter reaction that is the focus of this study. This is due to its obvious potential, as well as the relative ease with which it can be investigated by measuring acid consumption rates in simple leaching experiments. In contrast to most studies of mineral dissolution promoted by mechanical activation, this study focuses on the initial dissolution rates as a measure of surface reactivity rather than the time required to achieve a given degree of dissolution.

2. Materials and methods

2.1. The olivine

The olivine crystals used in this study were kindly supplied by the Norwegian mining company North Cape Minerals (NCM) and originate from the dunite deposit at Åheim in Western Norway. After a sample of pure and well defined crystals had been retrieved at Åheim, the material was gently crushed and sieved to obtain the 1–2 mm fraction. This fraction was then used directly as feed in the mechanical activation process without any further treatment.

The chemical composition of the olivine crystals was obtained from X-ray fluorescence (XRF) analysis performed on a sample from the 1–2 mm fraction using a *Phillips 1480* X-ray spectrometer. Normalisation of the analytical data produced the following olivine formula:

$$Mg_{1.860}Fe_{0.134}Ni_{0.006}SiO_4.$$

This is in close agreement with analysis reported by Osland (1998) and Jonckbloedt (1998). The results show that pure olivine from Åheim contains approximately 93 mol% forsterite (Mg_2SiO_4) and 7% fayalite (Fe_2SiO_4). This particular olivine composition is referred to as Fo_{93}.

2.2. Characterisation of milled/activated products

Size distributions of the activated olivine material were obtained from Frauenhofer diffraction analysis using a *Coulter LS 230 Particle Size Analyser*, whereas specific surface area was determined using the N_2-adsorption technique (i.e. the BET equation (Brunauer et al., 1938)) and a *Flow Sorb II 2300* volumetric gas adsorption analyser.

The activated olivine products were also characterised using scanning electron microscopy (SEM) and X-ray powder diffraction (XRD). The SEM images were obtained with the secondary electron detector using a Hitachi S-4300SE field emission SEM, whereas the XRD analysis was performed using a *Philips PW1710* diffractometer with a *PW 1830* generator, scanning from 2° to 60° using monochromatised CuK_α radiation. In order to obtain a reference point for the activated olivine materials, an XRD analysis was also performed on the fines (−200 μm) obtained from the initial crushing of the olivine crystals.

2.3. Mechanical activation

Mechanical activation of the olivine crystals was achieved using a *Fritsch Pulverisette 6* planetary mono mill by milling 12.9 g of the material in a 250 ml stainless steel mill chamber for various lengths of time. The milling was conduced at 500 rpm using twenty Ø20 mm stainless steel balls with a total weight of 645 g, thus yielding a grinding media to material ratio of 50.

The materials produced by milling in the planetary mill are referred to as *activated olivine* (*AOX*) with a further

reference to the activation time, e.g. the notation *AOX:15* represents olivine crystals that have been milled/activated for 15 min. The milling or activation time spanned from 1 to 60 min. The temperature of the activated olivine in the mill chamber was measured immediately after production using an IR-sensor. The temperature rose rapidly during milling, reaching almost 70 °C after 30 min. To prevent excessively high temperatures from occurring, no batch was subjected to more than 30 min of continuous milling. The *AOX:60* material was produced in two runs, separated by a 30 min cooling interval.

2.4. Leaching experiments

Leaching experiments were performed in a glass container (chemical reactor) at 25 ± 0.1 °C by exposing a carefully weighed amount of activated olivine to 100 ml of a solution containing 0.01 M HNO_3. Depending on the activation time of the milling products, the activated olivine was added at a dose ranging from 1 g/l to 20 g/l. The resulting suspension was stirred continuously using a magnetic stirrer operated at 500 rpm, while the pH of the system was measured and recorded automatically at preset intervals using a using a *Meterohm 713 pH Meter* and a *Aquatrode Plus* combined glass electrode (spherical bulb). The first pH reading was obtained 6 s after the start of the experiment. The pH meter was calibrated prior to each series of measurements, and great care was taken to minimise the risk of contamination throughout the study. All experimental runs were performed in duplicate.

A parallel set of experiments were conducted in which the leachate was sampled at various times during the leaching process by extracting and filtering a volume of 5 ml using a syringe and a 0.20 μm syringe filter. The filtrates were collected in glass vials and acidified using 20 μl of 65% nitric acid. Finally, the filtrates were analysed using the *inductively coupled plasma-mass spectroscopy* technique (ICP-MS) by a *Perkin Elmer DRCII ICP-MS* equipped with a dynamic reaction cell. Each determination was obtained by taking the average of three replicate measurements. Prior to analysis, all samples were diluted by a factor of 100.

3. Results and discussion

3.1. Results from the characterisation of milled/activated products

In addition to the primary or initial comminution effects, the size distribution and the specific surface of the activated products will also depend on secondary processes like aggregation and agglomeration (Juhász, 1974). The size distributions of the *AOX:5*, *AOX:15* and *AOX:60* materials are given in Fig. 1, whereas Fig. 2 shows the specific surface area S_{BET} as function of milling/activation time t_M. Results from the specific surface area analysis are also given in Table 1.

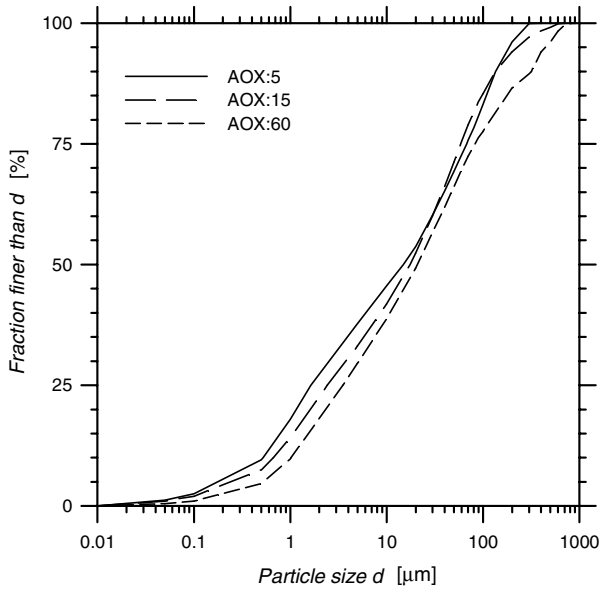

Fig. 1. Cumulative particle size distributions of selected activated olivine materials.

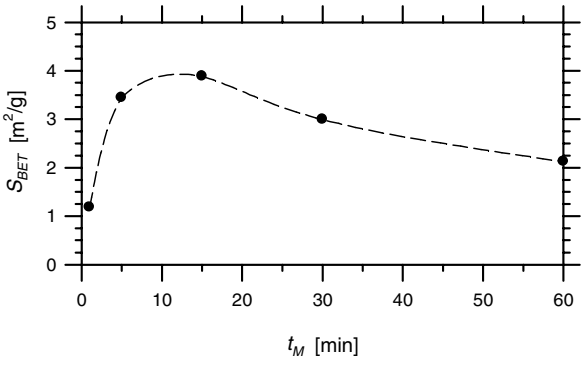

Fig. 2. Specific surface area S_{BET} as a function of milling time t_M.

Table 1
Average specific rate constants κ obtained from regression analysis as shown in Fig. 8. The corresponding R^2 values and the dose levels D upon which the regression is based are also given along with specific surface area S_{BET}

Product	κ [10^{-3} s^{-1}]	S_{BET} [m^2/g]	R^2	D [g/l]
AOX:1	0.9	1.18	0.998	10 and 20
AOX:5	1.5	3.44	0.959	5 and 10
AOX:15	2.3	3.88	1.000	2 and 5
AOX:30	4.7	2.99	0.985	1, 2 and 5
AOX:60	8.2	2.12	0.994	1 and 2

Fig. 1 shows how the particle size distribution is shifted to the right with increasing activation or milling time. The highest proportion of fines can be found in the *AOX:5* material. This corresponds well with the observed development in specific surface area even though the latter parameter peaks somewhat later at approximately 15 min of milling. As seen in Fig. 2, milling beyond this point does not produce a further net increase in surface area. Instead,

a significant decrease is observed. This behaviour is common for dry milling, and is usually explained by agglomeration of structurally modified particles following the initial reduction of particle size. This view is supported both by the shift in particle size distributions as well as the by the results of the SEM analysis, which clearly shows how prolonged milling results in an increasing degree of agglomeration and reduced amount of fines. The analysis reveals that distinct agglomerates are present in the fine fraction even after just 5 min of activation, but also that a significant part of the coarser fractions of the *AOX:5* material consists of discrete angular particles (Fig. 3a and b). In contrast, the coarser fractions of the *AOX:30* material consist entirely of agglomerates. However, sharp angular particles up to 2–3 μm in size can still be found as part of the larger agglomerates, thus demonstrating how the finest olivine particles are very resistant to milling (Fig. 3c and d).

The results from the XRD analysis show a large reduction in peak height and signal to noise ratio with increasing activation time (Fig. 4). The reduction is accompanied by a general broadening of the peaks. This is illustrated by Fig. 5, showing the development of the *Full-With-Half-Maximum* (*FWHM*) value of the 130 (*hkl*) peak shown in Fig. 4. Even though the results suggest structural modification and partial amorphisation of the olivine lattice, the presence of small but significant peaks even after 60 min of intense milling in the planetary mill can be taken as a further indication of the high milling resistance and mechanical strength of the submicron olivine particles.

3.2. Results from the leaching tests

The dissolution of olivine in acid has been studied by a number of investigators (Sanemasa et al., 1972; Luce et al., 1972; Blum and Lasaga, 1988; van Herk et al., 1989; Wogelius and Walther, 1991, 1992; Jonckbloedt, 1998). The initial phase of olivine dissolution in nitric acid can be described by the following equation:

$$(\mathrm{Mg,Fe})_2\mathrm{SiO}_{4(s)} + 4\mathrm{H}^+ \rightarrow 2(\mathrm{Mg}^{2+}, \mathrm{Fe}^{2+}) + \mathrm{H_4SiO_4^0}. \quad (1)$$

During dissolution in acid the olivine cations are replaced by hydrogen ions, yielding $\mathrm{H_4SiO_4^0}$ monomers and Mg^{2+} and Fe^{2+} ions in solution. Consequently, the reaction results in a net stoichiometric reduction of acidity. The resulting concentration of hydrogen ions in solution can be calculated from the measured pH. The relative acid consumption β can then be defined as the proportion of the amount of acid initially present that has been consumed by the olivine dissolution reaction:

$$\beta = \frac{[\mathrm{H}^+]_{\mathrm{ini}} - \frac{1}{\gamma} \cdot 10^{-\mathrm{pH}}}{[\mathrm{H}^+]_{\mathrm{ini}}}, \quad (2)$$

where $[\mathrm{H}^+]_{\mathrm{ini}}$ represents the initial acid concentration (i.e. 0.01 M), whereas γ is the activity coefficient of the hydrogen ions which was assumed equal to 0.9.

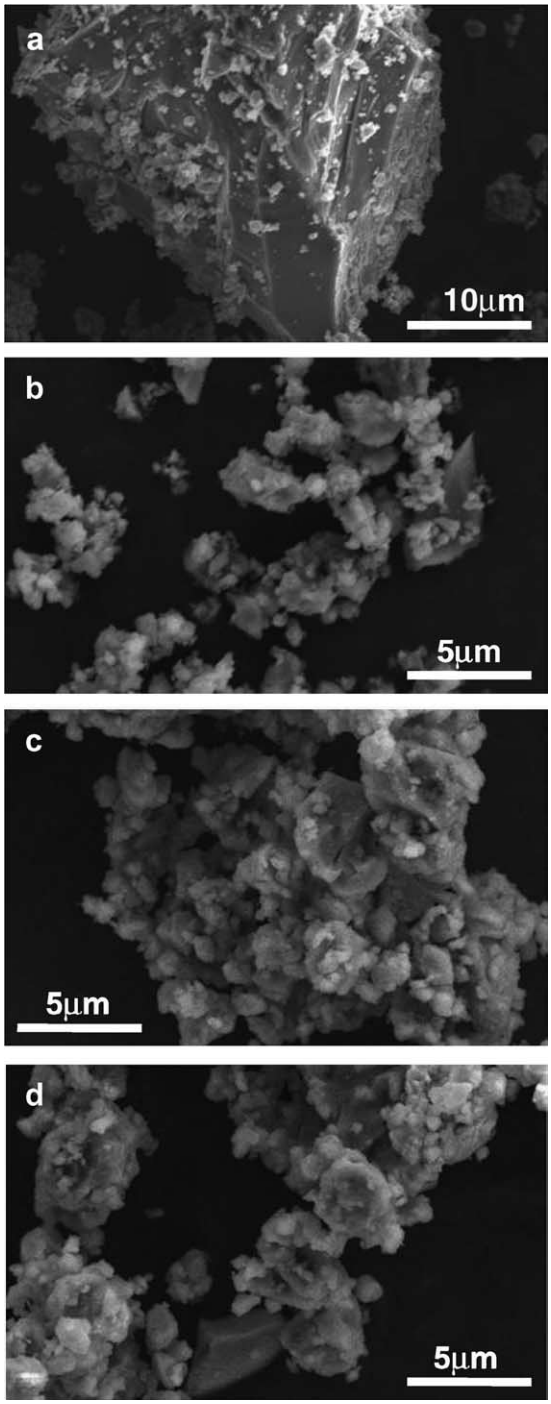

Fig. 3. Scanning electron microscope images of two different activated olivine materials: *AOX:5* (image a and b) and *AOX:30* (image c and d).

Following olivine dissolution, the concentrations of iron and silica in solution will increase and oxidation and precipitation reactions will inevitably occur. This will interfere with the acid budget and add to the complexity of the system. However, at the initial phase of the experiment these factors are negligible. This is illustrated in Fig. 6, which shows the concentration of magnesium and iron in the leachate as a function of the relative acid consumption for two different activated olivine materials. The actual

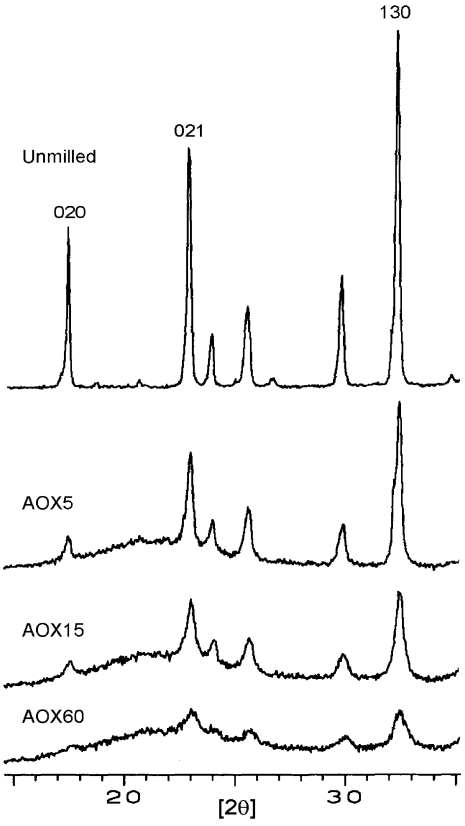

Fig. 4. Diffractograms (selected interval) comparing the XRD signature of the unmilled olivine crystals to those of the *AOX:5*, *AOX:15* and *AOX:60* materials.

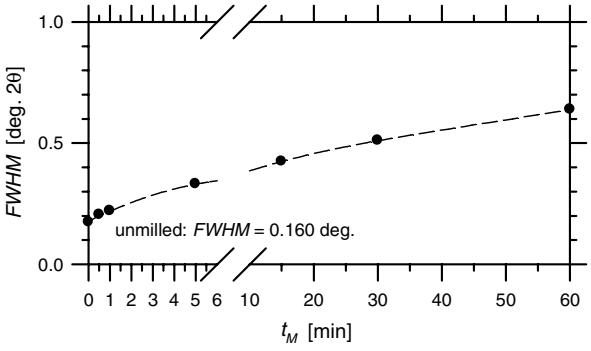

Fig. 5. Full-with-half-maximum (*FWHM*) for the 130 (*hkl*) peak as a function of activation time t_M.

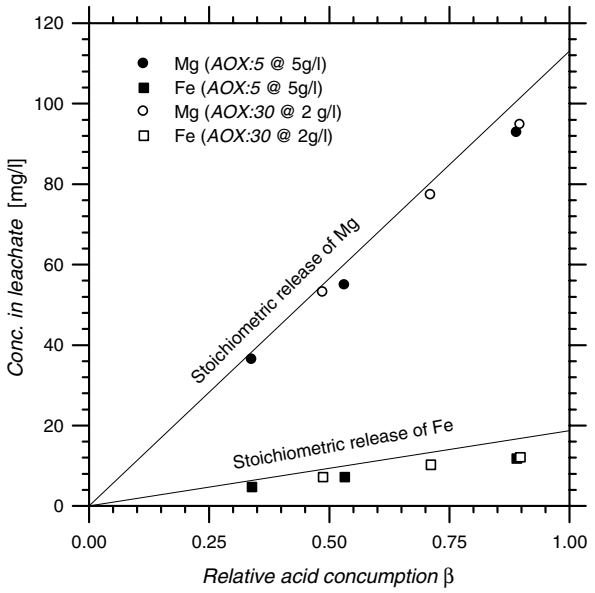

Fig. 6. Concentration of Mg and Fe in the leachate as a function of the relative acid consumption for two different activated olivine materials at specific dose levels. The solid curves represent the theoretically calculated stoichiometric release of Mg and Fe from Fo_{93}.

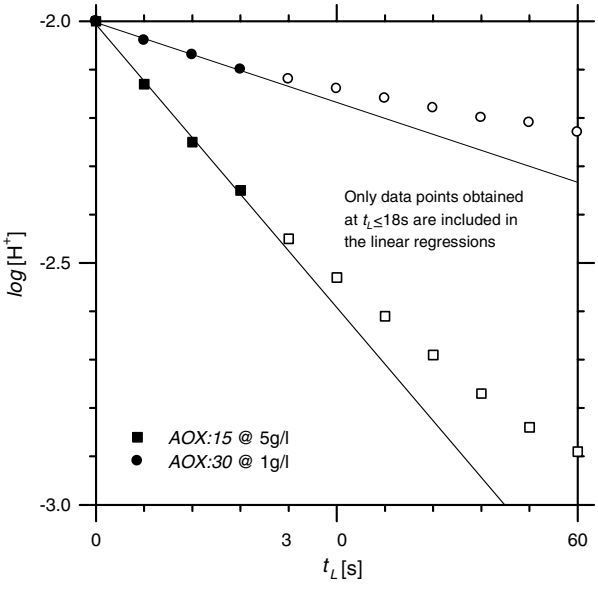

Fig. 7. Examples of plots of $\log[H^+]$ versus leaching time t_L for different activated olivine materials at specific dose levels.

concentrations correspond well with the theoretical curves for stoichiometric leaching of Fo_{93} both for the *AOX:5* and the *AOX:30* materials.

Preliminary experiments as well as the results shown in Figs. 6 and 7 demonstrate that the initial stage of the olivine dissolution reaction can be described by Eq. (1) and first order kinetics. Hence, the reaction rate r can be defined as

$$r = -\frac{\partial[H^+]}{\partial t} = k[H^+] = \kappa(D \cdot S_{BET})[H^+], \quad (3)$$

where k is the overall rate constant (s^{-1}), κ represents the *intrinsic* or *specific* rate constant [$l\,m^{-2}\,s^{-1}$] and D represents the olivine dose [g/l], i.e. $(D \cdot S_{BET})$ represents 'the extent of the system'. In order to quantify the reactivity of the different activated olivine products the rate constants were calculated from the experimental data. This was done as demonstrated in Fig. 7 by plotting the logarithm of the acid concentration ($\log[H^+]$) versus leaching time (t_L) and fitting a linear 'least squares' regression line through the origin and the first three data points (i.e. up to 18 s). The

overall rate constant k and the specific rate constant κ can then be found as the slope of the regression line multiplied by the factors $(-\ln 10)$ and $(-\ln 10/D \cdot S_{\mathrm{BET}})$, respectively.

Basing the regression line on three points and the origin is a compromise between data support and the validity of the fundamental assumptions regarding the overall reaction. As can be seen from the examples in Fig. 7, the fit to the regression line is good during the first 18 s, hence the results comply with first order kinetics within the chosen limited timeframe. As the purpose of this study is to investigate the *relative initial surface reactivity* of the activated olivine materials as a function of activation time rather than explaining the mechanisms of their dissolution in acid, the kinetic model in itself is not important as long as it is capable of describing and quantifying the initial reaction rates. It is also worth noticing that a significant amount of olivine is dissolved during the first 18 s of the reaction. The relative amount of olivine dissolved during this phase varies from 0.6% for the *AOX:1* material added at 20 g/l to 9.4% for the *AOX:60* material added at 1 g/l.

Fundamental kinetics implies that the initial reaction rate should be proportional to the initial total surface area, i.e. the same specific rate constant κ should be obtained for all the activated olivine products if the difference in their reactivity can be attributed solely to the variation in specific surface area. Slight variations in the specific rate constants were found for each of the activated olivine products when the constants were obtained at different dose levels. To obtain an average value for each product to facilitate comparison, the experimentally obtained overall rate constants k were plotted against the corresponding total surface area of the systems (i.e. as $D \cdot S_{\mathrm{BET}}$) as shown in Fig. 8. The slopes of the 'least squares' regression lines fitted to the data for each activated product then yield the corresponding average specific rate constant κ. As demonstrated in Fig. 8 and by the corresponding data given in Table 1, the value of the specific rate constant increases with increasing activation time, thus indicating an increase in reactivity that can not be explained by surface area measurements alone. To exemplify, the specific rate constant of the *AOX:60* material is 9.0 times higher than that of the *AOX:1* product, whereas the corresponding ratio between their specific surface areas is only 1.8, i.e. the reactivity appears to have been increased by a factor of approximately 5 due to structural effects alone.

3.3. Further discussion of the results

The results from the leaching experiments demonstrate how the observed variation in reactivity between the activated olivine products can not be accounted for by the corresponding variation in specific surface area values as obtained from the BET analysis. The absence of a simple proportionality between the S_{BET} parameter and the initial reaction rates could be seen as a strong indication of structural modification or activation of the olivine surfaces. This is supported by the results from the XRD analysis.

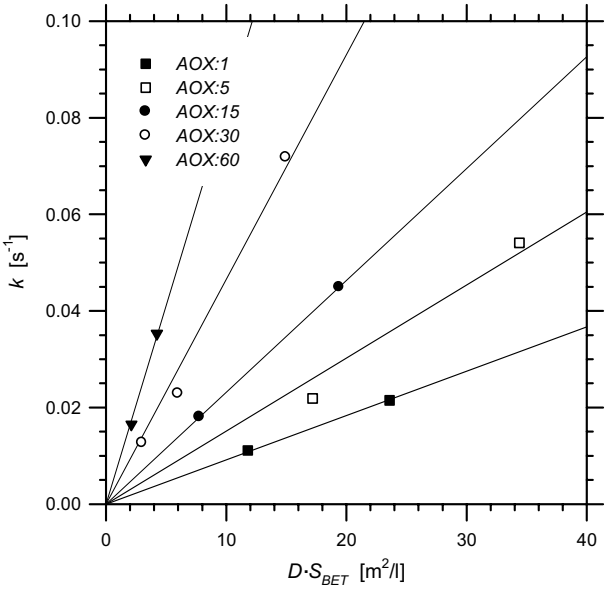

Fig. 8. Plots of overall rate constants k versus $D \cdot S_{\mathrm{BET}}$ for each activated olivine product. The respective average specific rate constants κ are given by the slopes of the linear regression lines. Data from the regression analysis are given in Table 1.

Alternatively, if we assume that the surfaces have been modified only to a minor extent, the specific surface areas obtained from the BET analysis performed on dry powders can not be representative for the effective surface areas in solution during the olivine dissolution reaction. Such a situation could be caused by rapid breakdown of the aggregates observed in the SEM images when the products are exposed to acid, thereby creating a larger effective surface area. However, the amount of acid required to achieve de-agglomeration must be relatively low and the process must occur more or less instantaneously. If this was not the case, the total effective surface area of the system would display significant variation throughout the course of acid consumption. As illustrated by the linear regression in Fig. 8, the good agreement between specific rate constants obtained from leaching experiments performed at different dose levels strongly suggests that the total surface area is fairly constant during the first 18 s of the dissolution reaction.

The results from both the leaching experiments and the XRD analysis suggest that the observed over-proportional increase in reactivity is largely due to structural disordering (i.e. mechanical activation) of the olivine surfaces, although the presence of large agglomerates partly consisting of angular submicron particles as shown by the SEM analysis raises questions regarding the effective surface area of the systems and how well this parameter is represented by the BET measurements. Further work is required in order to quantify the relative importance of structural disordering and the potential difference between BET surface area and effective surface area.

Regardless of the mechanisms at play, prolonged milling of olivine can cause a substantial increase in the surface

reactivity of the mineral when evaluated on a weight or volume basis. The experimental procedures presented in this paper are capable of revealing clear differences between the various olivine products with respect to their overall structure and their reactivity at the initial phase of the dissolution reaction. The results show that it is impossible to predict the relative reactivity of the activated olivine materials based on the BET surface areas alone. Further development of these procedures could represent a cost-efficient strategy for initial screening and characterising the effect of mechanical activation on surface reactivity, as well as yielding a basis for comparison of the different equipment used for activating minerals.

Further research and development of the various concepts based on mechanically activated olivine will proceed along two main paths. Firstly, in order to facilitate more specific studies of the individual concepts, it is necessary to develop tests designed to determine the reactivity of the activated products with respect to a range of potentially interesting surface reactions rather than just dissolution alone. The structural modifications responsible for increasing the reaction rates with respect to leaching could affect the reaction rates of heavy metal adsorption or carbon dioxide sequestration very differently. Consequently, the reactivity should be tested with respect to the specific reactions in question. Secondly, if the technology is to be employed at an industrial scale, it is necessary to evaluate the performance of scalable grinding equipment such as attritors, ball mills and nutating mills in order to assess the overall feasibility of the proposed concepts.

4. Conclusions

Prolonged dry milling of pure olivine crystals in a *Fritsch Pulverisette 6* planetary mono resulted in the agglomeration of partially structurally modified particles accompanied by a reduction in the amount of fines following the initial reduction of particle size. The coarser fractions of olivine subjected to 5 min of milling contained both agglomerates and discrete angular particles, whereas the latter was completely absent in the coarser fractions of materials milled for 30 min. However, sharp angular particles up to 2–3 μm in size could still be found as part of the larger agglomerates.

The specific surface area as obtained by BET measurements displayed an initial rapid increase as a function of milling time before it peaked at 3.88 m^2/g after 15 min and slowly decreased or levelled out.

Prolonged dry milling of pure olivine crystals resulted in products that were more reactive with respect to dissolution in acid than their respective BET surface areas would suggest. The initial phase of olivine dissolution could be modelled using first order kinetics. Relative to olivine that had been milled for 1 min, 60 min of milling increased the initial reaction rate by a factor of 9.0, whereas the corresponding increase in specific surface area was 1.8.

The results from both the leaching experiments and the XRD analysis suggest that the observed over-proportional increase in reactivity is largely due to structural disordering (i.e. mechanical activation) of the olivine surfaces, although part of the over-proportionality could be explained as differences between the true effective surface area of the systems and the values estimated by the BET measurements.

References

Baláž, P., 2000. Extractive Metallurgy of Activated Minerals. Elsevier, Amsterdam.

Baláž, P., 2003. Mechanical activation in hydrometallurgy. International Journal of Mineral Processing 72, 341–354.

Blum, A., Lasaga, A., 1988. Role of surface speciation in the low-temperature dissolution of minerals. Nature 331, 431–433.

Brunauer, S., Emmet, P.H., Teller, E., 1938. Adsorption of gases in multimolecular layers. Journal of the American Chemical Society 60, 309–319.

Harben, P.W., 2002. The Industrial Minerals Handybook, fourth ed. Industrial Minerals Information Ltd., London.

Huijgen, W.J.J., Comans, R.N.J., 2003. Carbon dioxide sequestration by mineral carbonation—Literature review. ECN-C–03-016, February 2003.

Jonckbloedt, R.C.L., 1998. Olivine dissolution in sulphuric acid at elevated temperatures: implications for the olivine process, an alternative waste acid neutralizing process. Journal of Geochemical Exploration 62, 337–346.

Juhász, A.Z., 1974. Mechanochemical activation of silicate minerals by dry fine grinding. Aufbereitungs-Technik 10, 558–562.

Kalinkin, A.M., Kalinkina, E.V., Makarov, V.N., 2003. Mechanical activation of natural titanite and its influence on the mineral decomposition. International Journal of Mineral Processing 69, 143–155.

Kalinkina, E.V., Kalinkin, A.M., Forsling, A.M., Makarov, V.N., 2001a. Sorption of atmospheric carbon dioxide and structural changes of Ca and Mg silicates during grinding: I. Diopside. International Journal of Mineral Processing 61, 273–288.

Kalinkina, E.V., Kalinkin, A.M., Forsling, A.M., Makarov, V.N., 2001b. Sorption of atmospheric carbon dioxide and structural changes of Ca and Mg silicates during grinding: II. Enstatite, åkermanite and wollastonite. International Journal of Mineral Processing 61, 289–299.

Kleiv, R.A., 2001. Heavy metal adsorption on silicate tailings—a study of nepheline syenite and olivine process dusts. Doctoral thesis, Norwegian University of Science and Technology, Trondheim, Norway, ISBN 82-471-5332-7.

Kleiv, R.A., Sandvik, K.L., 2002. Modelling copper adsorption on olivine process dust using a simple linear multivariable regression model. Minerals Engineering 15 (10), 737–744.

Kleiv, R.A., Sandvik, K.L., 2005. Mechanical activation of industrial minerals—new potential applications. In: Preprints, Konferens i Mineralteknik, 8–9 februari 2005 i Luleå, MinFo, Luleå, Sweden, pp. 87–95.

Kleiv, R.A., Thornhill, M., 2002. Initial neutralisation of acid mine drainage using magnesium olivine. In: Ciccu, R. (Ed.), SWEMP 2002—7th International Symposium on Environmental Issues and Waste Management in Energy and Mineral Production. DIGITA University of Cagliari, Italy, pp. 731–736.

Kleiv, R.A., Thornhill, M., 2004. Adsorptive retention of copper from acidic mine water at the disused sulphide mine at Løkken, central Norway—initial experiments using olivine. Minerals Engineering 17, 195–203.

Kleiv, R.A., Sandvik, K.L., Thornhill, M., 2001. Pre-treatment of acid mine drainage using magnesium olivine. In: Proceedings of Securing the Future—International Conference on Mining and the Environ-

ment, June 25–July 1, 2001, Skellefteå, Sweden, vol. 1. The Swedish Mining Association, Skellefteå, Sweden, pp. 336–342.

Kleiv, R.A., Sandvik, K.L., Rudi, F., 2002. Olivine in iron and steelmaking. In: Preprints: Second International Conference on the Iron Ore Industry: Today and Tomorrow (TIOITT-2002)–June 11–13, Kiruna, Sweden. LKAB/Luleå Universitet, Kiruna, Sweden.

Lackner, K.S., Wendt, C.H., Butt, D.P., Joyce Jr., E.L., Sharp, D.H., 1995. Carbon dioxide disposal in carbonate minerals. Energy 20, 1153–1170.

Lackner, K.S., Butt, D.P., Wendt, C.H., 1997. Progress on binding CO_2 in mineral substrates. Energy Conversion 38, 259–264.

Luce, R.W., Bartlett, R.W., Parks, G.A., 1972. Dissolution kinetics of magnesium silicates. Geochimica et Cosmochomica Acta 36, 35–50.

Morales, T.A., Herbert, R.B., 2001. Sulphur and iron chemistry in a barrier system for the remediation of groundwater contaminated by AMD; Kristineberg mine site, Nothern Sweden. In: Proceedings of Securing the Future—International Conference on Mining and the Environment, June 25–July 1, 2001, Skellefteå, Sweden, vol. 1. The Swedish Mining Association, Skellefteå, Sweden, pp. 546–555.

O'Connor, W.K., Dahlin, D.C., Nilsen, D.N., Rush, G.E., Walters, R.P., Turner, P.C., 2001. Carbon dioxide sequestration by direct mineral carbonation: results from recent studies and current status. In: Proceedings from the 1st National Conference on Carbon Sequestration, May 14–17, 2001, Washington DC.

Osland, R., 1998. Modelling of variations in Norwegian olivine deposits—causes of variations and estimation of key quality factors. Doctoral thesis, Norwegian University of Science and Technology, Trondheim, Norway, ISBN 82-471-0192-0.

Rudi, F., 2001. Olivine—a Norwegian forte. Industrial Minerals, November 2001.

Sanemasa, I., Yoshida, M., Ozawa, T., 1972. The dissolution of olivine in aqueous solutions of inorganic acids. Bulletin of the Chemical Society of Japan 45, 1741–1746.

Schuiling, R.D., 1986. A method for neutralizing waste sulfuric acid by adding a silicate. European Patent Application No. 8590353.5, Utrecht University, Netherlands.

Schuiling, R.D., 1998. Geochemical engineering; taking stock. Journal of Geochemical Exploration 62, 1–28.

van Herk, J., Pietersen, H.S., Schuiling, R.D., 1989. Neutralization of industrial waste acids with olivine—the dissolution of forsteritic olivine at 40 °C–70 °C. Chemical Geology 76, 341–352.

Wogelius, R.A., Walther, J.V., 1991. Olivine dissolution at 25 °C: effects of pH, CO_2 and organic acids. Geochimica et Cosmochimica Acta 55, 943–954.

Wogelius, R.A., Walther, J.V., 1992. Olivine dissolution kinetics at near-surface conditions. Chemical Geology 97, 101–112.